This is the Accepted version of the article; the final Published version of the paper can be accessed in the journal:

Fusion Engineering and Design, Volume 84, Issues 2–6, 2009, Pages 509-513, ISSN 0920-3796,

https://doi.org/10.1016/j.fusengdes.2008.12.078

Design of a beam dump for the IFMIF-EVEDA accelerator

B. Brañas[a,*], D. Iglesias[a], F. Arranz[a], G. Barrera[a], N. Casal[a], M. García [b,c], J. Gómez[a], D. López [b,c], J.I. Martínez[a], F. Martín-Fuertes[a], F. Ogando [b,c], C. Oliver[a], J. Sanz [b,c], P. Sauvan [b,c], A. Ibarra[a]

[a] *CIEMAT, Avda. Complutense 22, 28040 Madrid, Spain*
[b] *Dpto. Ingeniería Energética, UNED, 28040 Madrid, Spain*
[c] *Instituto de Fusión Nuclear, UPM, 28040 Madrid, Spain*

Abstract

The IFMIF-EVEDA accelerator will be a 9 MeV, 125mA cw deuteron accelerator prototype for verifying the validity of the accelerator design for IFMIF. A beam stop will be used for the RFQ and DTL commissioning as well as for the EVEDA accelerator tests. Therefore, this component must be designed to stop 5MeV and 9MeV deuteron beams with a maximum power of 1.13MW.

The first step of the design is the beam-facing material selection. The criteria used for this selection are low neutron production, low activation and good thermomechanical behavior. In this paper, the mechanical analysis and radioprotection calculations that have led to the choice of the main beam dump parameters will be described.

The present design is based on a conical beamstop (2.5 m length, 30 cm diameter, and 3.5 mmt hickness) made of copper plus a cylindrical 0.5 m long beam scraper. The cooling system is based on an axial high velocity flow of water. This design is compliant with the mechanical design rules during full power stationary operation of the accelerator. The radioprotection calculations performed demonstrate that, with an adequate local shielding, doses during beam on/off phases are below the limits.

Keywords:

Beam stop, Thermo-mechanical design

1. Introduction and design requirements

The IFMIF-EVEDA accelerator [1] will be a 9 MeV, 125mA cw deuteron accelerator, identical to the low energy section of one of the IFMIF accelerators, which will be tested to verify the validity of the design before launching the IFMIF construction. It includes an ion source, a Radiofrequency Quadrupole cavity and the first module of a superconducting linac based on half wave resonator cavities. As no target is foreseen for the accelerated beam, a beam dump is required to stop it during commissioning and accelerator tests.

To minimize the accelerator activation, the commissioning will be performed mainly with H_2^+ pulsed beams with progressively increasing duty factor and current up to the nominal 125 mA current. Therefore the beam dump must be able to stop deuteron and H_2^+ continuous and pulsed beams with energies 5MeV (RFQ commissioning) and 9MeV. The maximum beam power is 1.12MW corresponding to a beam current of 125mA. A maximum operation time at full current of D+ of around 1 year and an operation time with 5Hz pulsed beam with 0.1% duty cycle of 2 months have been assumed.

As the range of 9 MeV deuterons in the possible candidate materials is of the order of hundreds of microns, it is not possible to install a vacuum window previous to the beam dump. Therefore the beam dump must operate in vacuum.

The beam dump and its surroundings will become activated due to neutron irradiation coming from deuteron reactions with the beam dump material and the beam facing material itself will be highly activated by the neutrons and the impinging deuterons. This implies that the beam stop geometry and materials must be chosen carefully and that the beam stop must be surrounded by a local shielding. The design must be such that the following requirements are fulfilled:

- Dose values outside the accelerator vault during accelerator operation must be below the acceptable levels for workers.

- Man access to the accelerator vault must be allowed for maintenance during beam-off phases.

- At the end of the EVEDA tests the beam dump must be qualified for a suitable waste management option such as shallow burial or near surface disposal.

2. Thermal management: geometry choice

The power density incident on the beam dump material surface determines the mean temperature and temperature gradients inside the target material and therefore the value of the thermomechanical stresses. The higher the power density the larger the thermal stresses and the heat transfer rate to the coolant, and consequently the beam dump complexity. Therefore it is important to reduce the maximum deposited power density as much as possible. This can be achieved by defocusing the beam to increase its size and by using very low incidence angles in the beam stop thus maximizing the material surface hit by the beam.

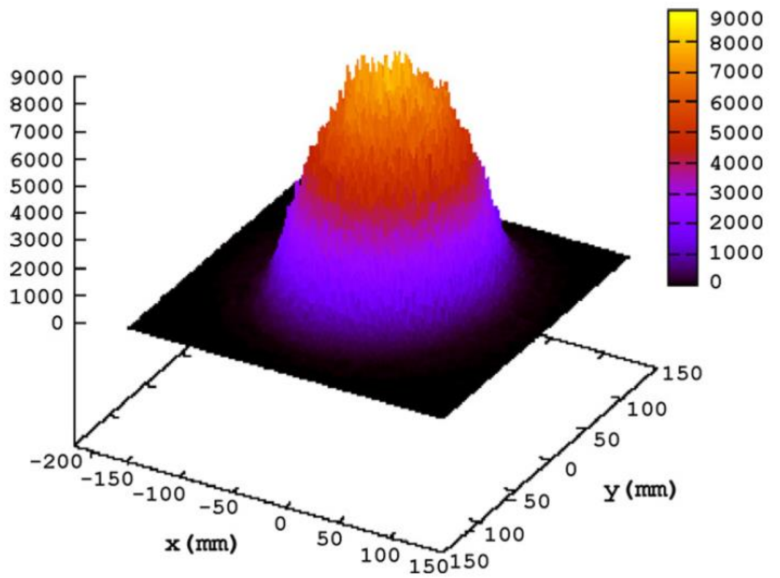

Fig. 1. Beam profile (W/cm2) at the beam dump entrance. z = 0 is taken at the cone

The beam, which has a rms radius of 3mm at the accelerator exit, is opened by the action of three quadrupoles whose currents and positions have been chosen to obtain the highest possible beam size (42mm) and divergence (15mm/m) at the beam dump entrance. The resultant beam profile departs from a Gaussian being less peaked and with less power at the edges (see Fig. 1).

After analyzing the behavior of different beam stop surface shapes [2] a conical shape has been chosen. This shape is adequate for an almost axi-symmetric beam as the one we have. On the other hand it takes advantage of the beam divergence because the more central (and dense) regions of the beam are intercepted after the beam has diverged along the beam dump. The resulting beam deposition profile shows a maximum (Fig. 2).

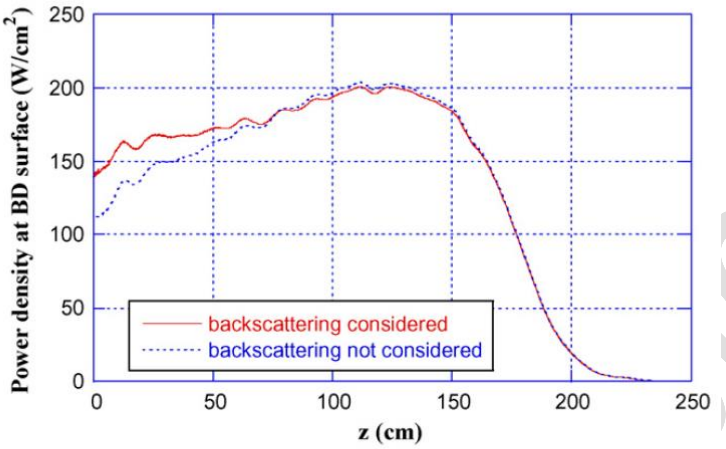

Fig. 2 Power density profile on a conical beam dump (L = 2.5 m, R=15cm). The dotted line represents the total incident power density whereas the continuous line represents the real absorbed power density taking into account the effect of backscattering

Taking into account previous experiences and the space availability, a length of 2.5 m was chosen. With regard to the diameter, on one hand it must be small to present a low incidence angle to the beam and to minimize the radiation doses but on the other hand it must be enough to contain the whole beam including the halo (for Gaussian beams an aperture of five times the rms size is normally used). By adding a 50 cm cylindrical scraper in the beam diverging region in front of the beam dump the cone aperture diameter of 30cm can fulfil all these requirements.

The power deposited at the beam dump surface has been calculated using the particle position and velocity distributions at the beam dump entrance obtained from the beam dynamics simulations of the high energy beam transport line [3]. The effect of the ion backscattering at the beam dump surface cannot be neglected at the low incidence angles (around 3◦) of our case and it has been calculated using the information on number, angle and energy of backscattered ions obtained from the SRIM code [4]. As it is shown in Fig. 2, this effect leads to a modification of the final energy deposition profile which results in a power density increase near the cone tip.

3. Cooling system

The heat transfer in the beam dump takes place in two almost uncoupled steps:

1. The heat transmission from the beam-facing surface through the material, which is governed by the material conductivity *K*. The temperature difference between the beam-facing and coolant facing surfaces depends on *K* and material thickness but it is independent of the cooling system.

2. The heat transfer from the material to the coolant, which is governed by the film coefficient *h*. This coefficient and the temperature of the material in contact with the coolant depend on the coolant flow conditions, being independent of the material properties.

A scheme with axial flow through the annular cross-section between two concentrical cones (in a similar manner to that of the LEDA [5] or IPHI beam dumps) has been considered. The coolant channel geometry is chosen to obtain sufficient velocity in the high power density zone, avoiding too high values which can produce vibrations and material erosion and too low ones which would cause a poor heat transfer. A high velocity is needed specially at the regions of higher power deposition (first half of the beam dump) where a large heat transfer rate between material and coolant is required to limit the coolant–material interface temperature and consequently the required water pressure. The water enters at high velocity (5 m/s) at the cone vertex and flows in counter-beam direction. To maintain the velocity along the beam dump it is necessary to reduce the coolant channel width progressively to compensate the increasing cone radius. Fig. 3 shows the geometry of the coolant channel that has been chosen. In this scheme the water flows between the internal cone and the external tube which is made of three cones with different slopes.

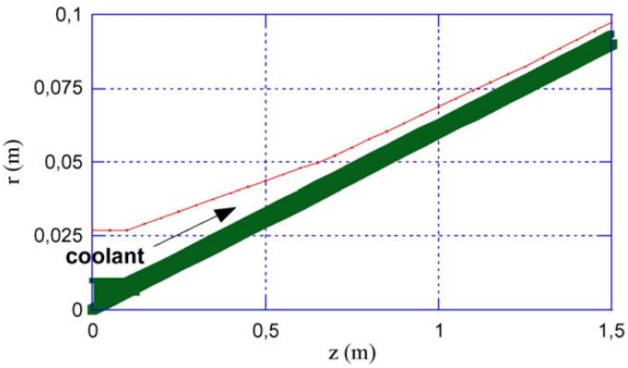

Fig. 3 Coolant channel geometry.

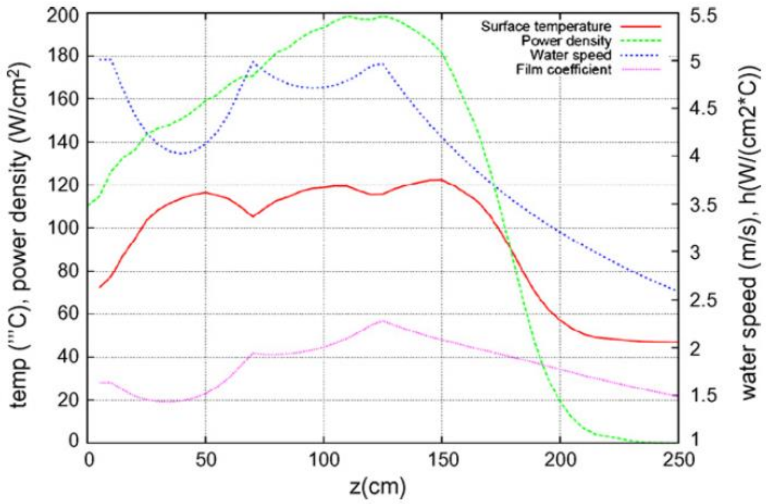

Fig. 4 Temperature of coolant-facing surface, water velocity, film coefficient and power density along the beam dump. z = 0 corresponds to the cone vertex.

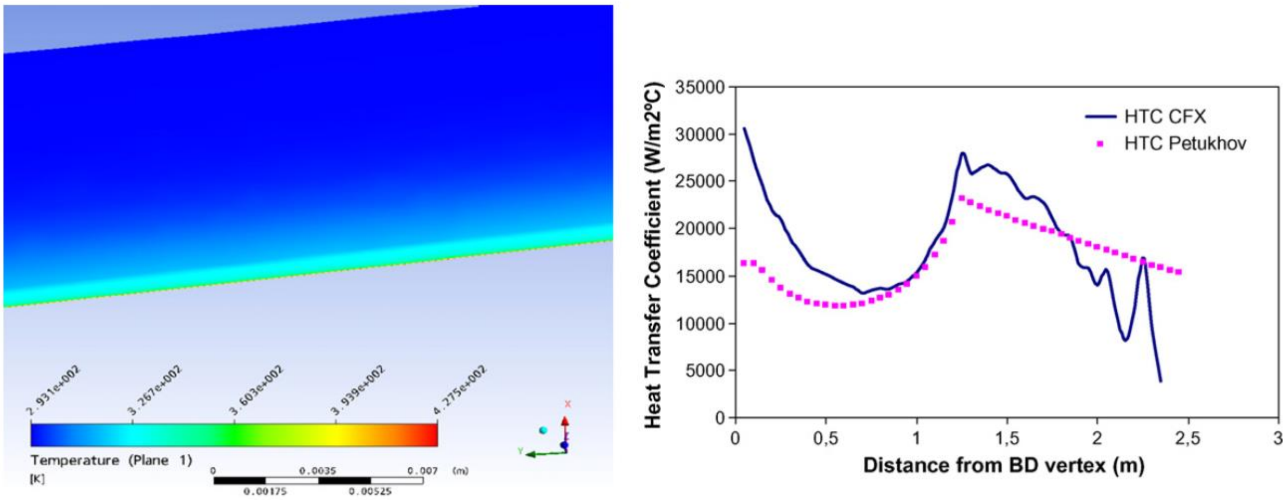

Fig. 5 (a) Temperaturemap in the fluid calculated with CFX and (b) corresponding heat transmission coefficient and comparison with the one obtained with the correlation.

A 10 kg/s coolant mass flow and 20 ºC coolant inlet temperature have been considered. To start with, a 1D heat transfer analysis has been performed (which is a good approximation given the symmetry of the problem, the fact that the cone thickness is much lower than its radius and the almost radial temperature gradients). Fig. 4 shows the calculated coolant temperature and that of the beam dump surface in contact with the coolant. *h* Values around 15,000–22,000 $W/m^2\ K$ are obtained using the Pethukov correlation. Given the high sensitivity of the results to the value of *h*, these estimations were cross-checked with the results of a fluid dynamic simulation performed with the CFX code. The *h* values inferred from the CFX temperature maps (see Fig. 5) are of the order of those calculated with the correlation.

The analysis performed shows that a cooling system based on liquid water flowing at high velocity is appropriate for this application. As the temperature of the material at the coolant side can reach 130 ºC, the water must be slightly pressurized (around 6 bar) to avoid local boiling. The pressure loss along the cone and in the whole circuit have been estimated to be around 1.5 bar and 2.5 bar respectively.

Table 1. Properties of different candidate materials.

	Density (kg/m^3)	Cp (J/kgK)	E (GPa)	Yield strength (MPa)	K (W/mK)	T_{fus} (◦C)	α (10^{-6} K^{-1}) 20–300 ºC	K/(E α) (10^{-3} W/m GPa)
Cu 101	8940	385	115	69-360	386	1083	17.7	192
Al 1050	2705	900	69	28-145	227	933	25.5	129
W	19300	130	398	520-725	166	5930	3.93	106
Ta	16000	140	186	475-730	57.5	2996	6.3	50
Ni 200	8900	440	204	148	90	1453	13.4	33

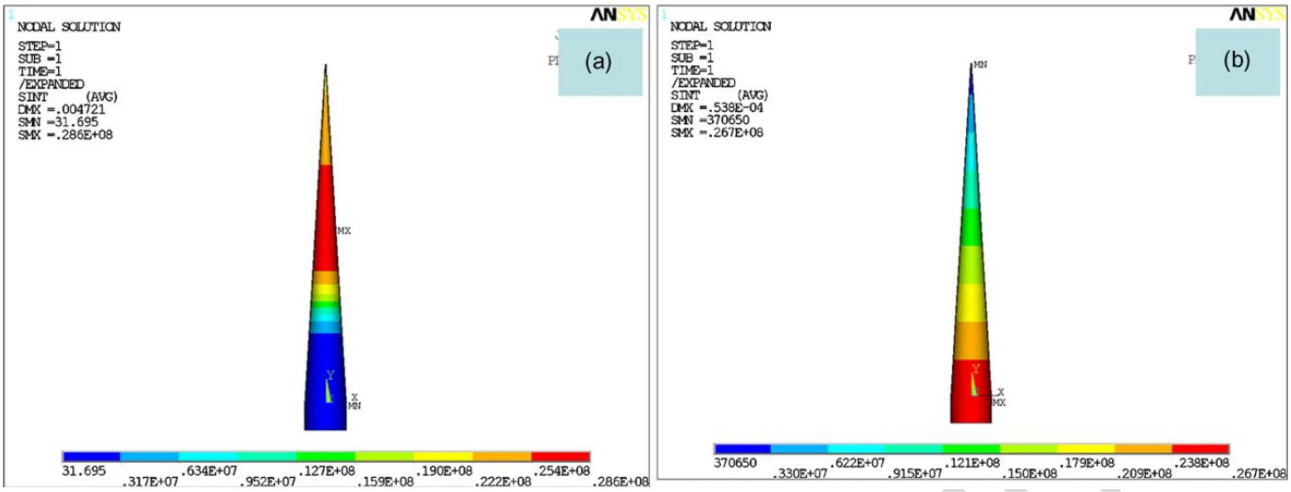

Fig. 6 Stress intensity on a Cu conical beam dump (L = 2.5 m, R = 15 cm, and 3.5mm thickness). (a) Thermal contribution. (b) Pressure contribution.

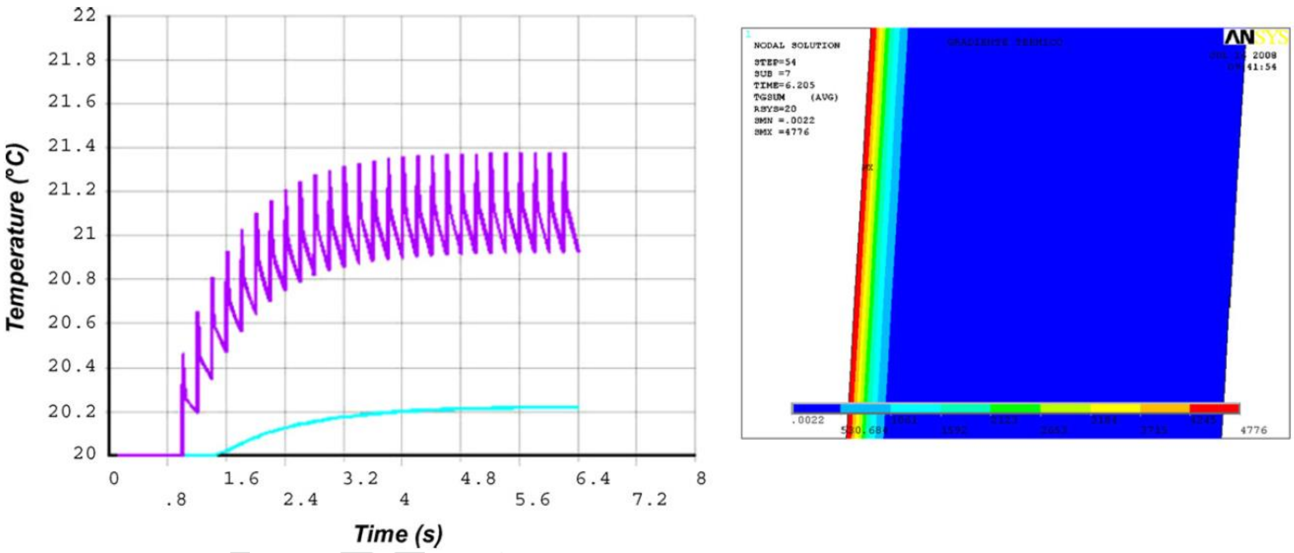

Fig. 7 Temperature evolution of coolant and material (inner surface) during pulsed operation. Map of thermal gradient at the time of maximum temperature.

4. Thermomechanical analysis

The structural behavior of the beam dump has been analysed with ANSYS during nominal full current stationary operation. The mechanical loads on the system are its weight, the coolant pressure and the thermal stresses produced by the thermal gradients. The analysis shows that the stresses depend strongly on the boundary conditions considered at the supports indicating that great care must be taken in their design. As the deuterons are stopped in the first 10 µm surface energy deposition is assumed.

The thermal stresses are proportional to the deposited power density and strongly dependent on the material. These stresses arise mainly by thermal expansion of the inner part of the beam dump which is constrained by the outer colder part. Therefore, the lower the expansion and the resistance to that expansion, the lower the stresses generated by the power deposition. So, for a given geometry and power density, the stresses are approximately proportional to the parameter ($E\ \alpha)/K$, where E is the Young modulus, α is the thermal expansion coefficient and K is the conductivity. Table 1 shows the main properties of different candidate beam dump materials.

Copper has been chosen as the material for the beam dump because it shows the lowest thermal stresses, its high ductility and the easier manufacture.

A beam dump thickness of 3.5 mm has been chosen. This choice comes from a compromise between the thermal stresses, which are almost proportional to this parameter, and the pressure stresses which have the opposite dependence.

Fig. 6 shows the thermal and pressure contributions of the stress intensity in the copper beam dump (L = 2.5 m, R = 15 cm, and 3.5 mm thickness). The maximum thermal stress occurs at a location close to that of the maximum power deposition ($z\sim$1.3 m). On the contrary, the pressure stresses increase with increasing cone radius, showing a maximum at the cone entrance. A total maximum stress of 43 MPa is obtained at an intermediate position. It has been checked that these stresses are compliant with the ASME design rules [6]:

P_m = 26.7 MPa < S_m

$P_m + Q$ = 43.3 MPa < 3 S_m

where P_m is the total primary membrane stress (due to pressure and weight loads), Q is the secondary thermal stress and S_m is defined as S_m =min(1/3 S_u, 2/3 S_y) = 34.5MPa being S_y and S_u the yield and tensile strengths at the working temperature.

The behavior of this beam dump under the accelerator commissioning pulsed operation has also been studied. Due to the low mean power (only 1 kW) the material temperature and its variation are very low. Fig. 7 shows the results obtained with ANSYS. Similar results have been also obtained using the 1D heat transfer module of the MELCOR 1.8.5 code. A maximum temperature gradient of 4776 K/m appears at the inner surface which is slightly lower than the one appearing during stationary full current operation. Therefore, using the stress and strain values obtained for the stationary full current case as an upper limit, it has been checked that no failure due to fatigue can be expected during the foreseen pulsed operation time of a few months.

5. Radioprotection analysis

A comparison of different materials from the radiological point of view has been performed. For the studied materials the values of neutron production vary in the range 10^{-4} to 10^{-3} neutrons per incident deuteron on a thick target (of the order of the stopping range) as can be seen in Fig. 8. W and Ta present the lowest neutron production. The slowing-down of deuterons according to SRIM and total neutron cross-section taken from the EAF library [7] have been used in the calculations. More details can be found in [8]. Most of the neutrons come from reactions between deuterons and the beam-stop material but there is a small contribution from reactions between the incident ions and implanted deuterium.

With the ACAB activation code [9] specific activity, contact dose rate, emitted photons, decay heat and waste disposal ratings (WDR) have been estimated. The energy and angle dependencies of the neutron flux have been calculated with MCNPX [10] and the total values have been scaled so that the total neutron flux corresponds to the one estimated with the EAF cross-sections. The contact dose values assuming a semi-infinite slab of material are presented in Fig. 9 for the cooling time following an irradiation period of 1 year. The conclusions of the study are that carbon has the lowest activation followed by Au, Ta and W. The specific activation produced by the deuterons is larger than that due to neutrons but it is restricted to the region where the deuterons penetrate (with a thickness of less than 10 μm taking into account the almost tangential incidence). Regarding waste assessment, considering only the volume activated by deuterons the

WDR are less than one (limit for near surface burial) for all materials except Ni, SS304L and Al and above all Zr (WDR much higher than 1). In the neutron-activated volume WDR much less than the limit are obtained for all the materials.

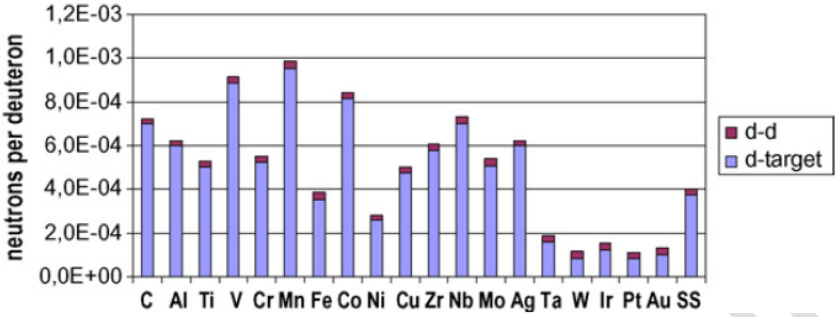

Fig. 8 Neutron production per incident deuteron for different materials.

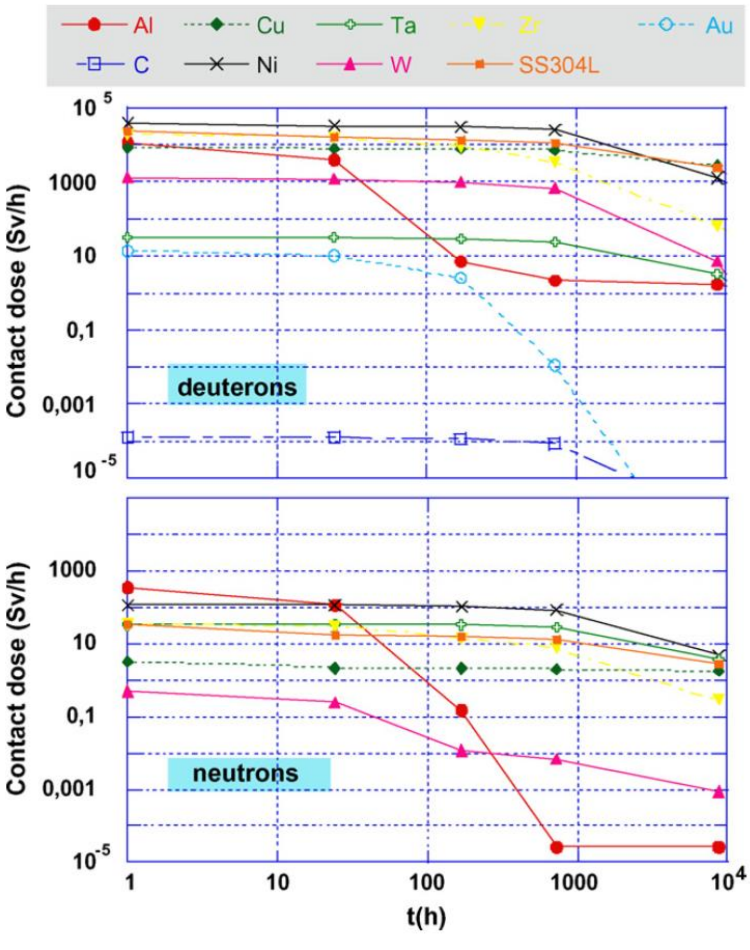

Fig. 9 Contact dose rates comparison for different beam facing materials.

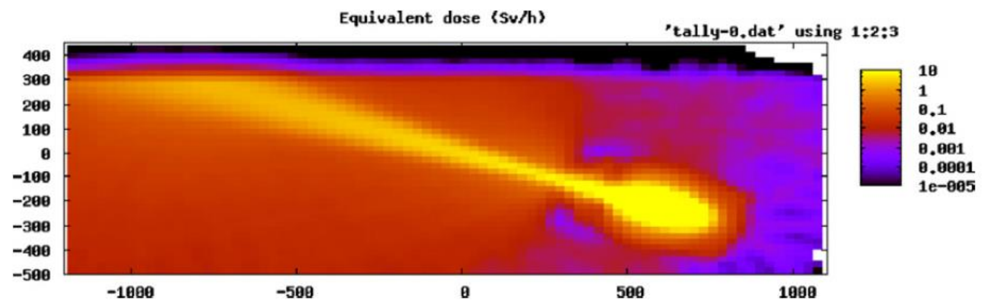

Fig. 10 Neutron dose inside the accelerator vault.

A local shielding must be set up around the beam dump. It will be made of a 1 m radius water tank to moderate the neutrons and a 1 m concrete wall. The calculations performed by MCNPX for the reference copper conical beam dump (2.5 m long, 30 cm diameter, 3.5 mm thickness, and 50 cm cylindrical scraper) with this local shielding show neutron doses during accelerator operation below 10 μSv/h outside the 1.5 m concrete thickness wall of the accelerator vault (Fig. 10).

To assure that doses inside the vault when the accelerator is not operating are below 10 μSv/h, especially in the neighbourhood of the beam dump wall, a lead plug must be installed to close the orifice made in the concrete for the beam tube. Once deuteron operation has started, the access to the interior of the concrete shielding walls will be possible but with restrictions, provided that the beam stop is shielded by the water tank.

6. Conclusions

A conceptual design has been proposed for the IFMIF-EVEDA accelerator beam dump. It is based on a conical beam stop (2.5m length, 30 cm diameter, and 3.5 mm thickness) made of copper plus a cylindrical 0.5 m long beam scraper. The cooling system is based on an axial high velocity flow of water.

This design has been shown to be compliant with the mechanical design rules during full power stationary operation of the accelerator.

The radioprotection calculations performed demonstrate that doses during beam on/off phases are below limits with an adequate local shielding.

References:

[1] A. Mosnier, A. Facco, A. Ibarra, Proceedings of the European Particle Accelerator Conference, 2008, p. 3539.

[2] B. Brañas, F. Arranz, G. Barrera, J.M. Gómez, A. Ibarra, D. Iglesias, et al., Proceedings of the European Particle Accelerator Conference, 2008, p. 259.

[3] C. Oliver, B. Brañas, A. Ibarra, I. Podadera, N. Chauvin, A. Mosnier, et al., Proceedings of the European Particle Accelerator Conference, 2008, p. 3041.

[4] SRIM. Stopping range of ions in matter. <http://www.srim.org>.

[5] T.H. Van Hagan, D.W. Doll, J.D. Schneider, F.R. Spinos, LINAC Conference Proceedings, 1998.

[6] ASME VIII. Div. 2. Pressure vessels.

[7] R.A. Forrest, The European activation file: EAF-2007 deuteron- and proton induced cross section libraries.

[8] J. Sanz, M. García, P. Sauvan, D. López, C. Moreno, A. Ibarra et al. Neutron induced activation in the EVEDA Accelerator materials: Implications for the accelerator maintenance, Journal of Nuclear Materials (2008), doi:10.1016/j.jnucmat.2008.12.277.

[9] J. Sanz, ACAB: Activation Code for Fusion Applications: User's Manual V5.0, Lawrence Livermore National Laboratory, UCRL-MA-143238, February 2000.

[10] MCNPX TM User's Manual, Version 2.5.0, LA-CP-05-0369, <http://mcnpx.lanl.gov>.